Adsorption of Sulfonamides on phosphorene quantum dots

J. W. Pino-Román, J. D. Correa, M. E. Mora-Ramos E. Flórez

1. Introduction

In recent years, the protection and conservation of water sources have gained enormous significance after decades of negligence in managing the waste produced by human activity. A particular case of this negligence is the biological waste generated by various industries and the rise of antibiotic consumption alongside the increasing human population, which for years has been directly discharged into the water bodies that supply both small and major cities.

Specifically, sulfonamide contamination in water bodies has been a concern, as these water-soluble compounds pose health and environmental risks to both human populations and non-target species [1].

Sulfonamides were discovered in the 1930s as a response to the need for antimicrobials to treat animal bacterial infections, given the increasing demand for animal protein food. After administration, sulfonamides are excreted via urine and feces, subsequently entering the aquatic environment through wastewater discharge, significantly contributing to antibiotic pollution. Despite their relatively low concentrations in environmental samples, measured in μg/L or ng/L, the continuous release of sulfonamides may pose risks to non-target species previously considered safe, as they can cause unknown effects despite being designed to target specific metabolic pathways, often leading to significant environmental implications [2].

The presence of these and various other environmental issues, such as air pollution, has created a need to clean and contribute to the restoration of our vital resources. This is where multiple studies have emerged, aiming to develop structures capable of detecting or adsorbing these pollutants, as their persistence in the environment, particularly in water and soil, poses significant ecological and health risks. Effective decontamination methods are crucial for mitigating these risks. Biochar, particularly when activated with metals like iron, has shown promise in removing sulfonamides from water and soil. Metal-free biochar derived from coconut shells can activate

peroxymonosulfate (PMS) to degrade sulfonamides like sulfamethoxazole (SMX) effectively, achieving up to 99% removal in chloride-rich environments [3]. Similarly, iron-activated biochar enhances the sorption of sulfanilamide in soils, reducing its bioavailability and movement, thus mitigating contamination [4].

The decontamination of sulfonamides using 2D materials is an emerging area of research, focusing on the development of advanced materials for efficient removal of these antibiotics from water systems. 2D materials, such as covalent triazine-based frameworks and graphitic carbon nitride, have been shown to enhance photocatalytic activity for the degradation of sulfonamides. These materials facilitate charge separation and transfer, leading to high degradation efficiencies under simulated solar light. For instance, a CTFNS/CNNS heterojunction was able to decompose sulfamethazine with a 95.8% efficiency, highlighting the potential of 2D/2D heterojunctions in wastewater treatment [5].

Due to their potential, in recent years there has been an increasing interest in the theoretical characterization of 2D materials [6]. For instance, 2D materials are also being utilized in the development of electrochemical immunosensors for the detection of sulfonamides. For example, 2D Cu-TCPP(Fe) has been used to create a highly sensitive sensor capable of detecting sulfonamides at low concentrations. This approach offers a wide detection range and high precision, making it suitable for environmental monitoring [7].

More recently, quantum dots have gained attention due to their vast number of potential applications. Phosphorene quantum dots [8] belong to a new class of zero-dimensional functional nanostructures with unique physicochemical surface properties compared to few-layer phosphorene and other 2D analogues. One of the most interesting applications is the adsorption of various molecules on these phosphorene quantum dots. PQDs are now considered promising catalytic materials for electrocatalytic water splitting and nitrogen reduction, lithium–sulfur batteries, solar light–driven energy devices, and biocatalysis, either in pristine form or as active components for constructing heterostructures with other 2D materials.
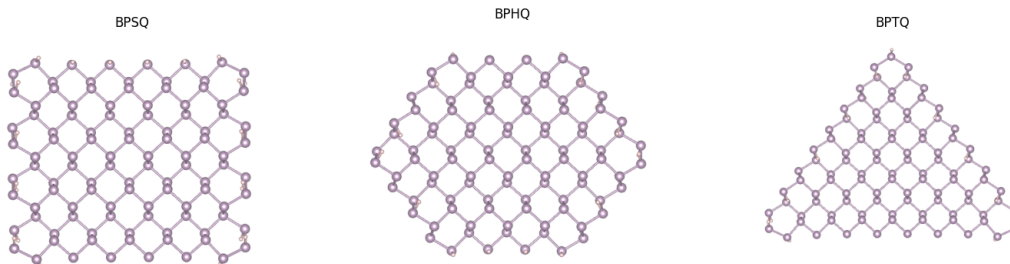
Figure 1: Quantum dot structures for adsorption assessment: Due to the structural differences among the three quantum dots, it is necessary to evaluate potential additional energy contributions from polarizations caused by the edges of each structure.

Motivated by the potential applications of quantum dots in molecule adsorption, we have conducted a systematic study of the electronic properties of phosphorene quantum dots and their adsorption energies for antibiotic contaminants present in water. The calculations were strengthened and corroborated through the use of different exchange-correlation functionals that included van der Waals interactions for adsorption both in the gaseous state and in the presence of a solvent.

2. Methods and Computational Details

The methodology employed in this study consists of four main steps: exploration of atomic sites, relaxation of structures, calculation of adsorption energies in gas, and calculation of adsorption energies in solvation.

2.1. Exploration of Atomic Sites:

Sulfonamides are characterized by two primary structural motifs: five-membered heterocyclic rings and six-membered cyclic structures. The study of sulfate radical-based oxidation processes has emphasized the crucial role of five-membered heterocyclic rings in the degradation of sulfonamides. Additionally, six-membered rings significantly influence the chemical behavior and degradation pathways of these compounds [9]. Therefore, our exploration focuses on variations in the positioning of these two structures.

To systematically explore adsorption sites, we developed a custom nomenclature for defining six atomic positions on quantum dots (QDs) interacting with sulfonamides. Each site is designated using the format QD-SF-PRS, where:

QD represents the abbreviated name of the quantum dot.

SF denotes the studied sulfonamide.

P indicates the atomic position.

R specifies the ring type, with values of 5 or 6, corresponding to whether the five- or six-membered ring is parallel to the quantum dot.

S defines the structural position, with values of 1 for top, 2 for bridge, and 3 for hollow sites.

For instance, a sulfamethoxazole molecule adsorbed on a triangular phosphorene quantum dot, where the five-membered ring is oriented parallel to the surface and positioned at a top site, is designated as BPTQ-SMX-P51. This classification framework enables a systematic and reproducible exploration of potential adsorption sites on phosphorene quantum dots. This process was conducted using the ASE framework [**?**], with the ASE-GUI toolkit for interactive atomic visualization.
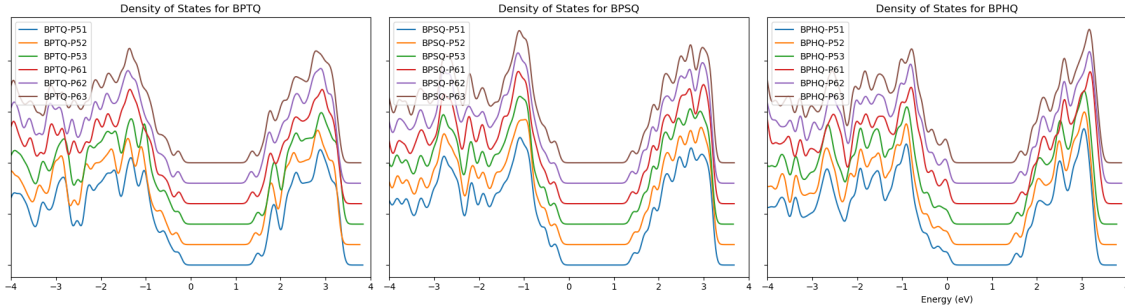

Figure 2: Comparison of the Density of States for the exploring sites: While all three structures exhibit similar general trends, differences in peak positions and intensities suggest variations in electronic properties, potentially influencing conductivity or optical behavior. The overall shape of the DOS curves indicates significant states around ±2–3 eV, with noticeable shifts between the materials, implying structural or compositional effects on their electronic characteristics.

2.2. Relaxation of Structures:

Structural relaxation in simulations is essential for accurately predicting adsorption properties, particularly in flexible frameworks such as metal-organic frameworks (MOFs). Rigid models often fail to capture the true adsorption behavior, especially at low concentrations [11]. To ensure the accuracy of our findings, all defined structures were subjected to relaxation using various computational calculators, allowing

4

them to reach their minimum energy configurations. This process is crucial for obtaining reliable adsorption energies and understanding the interactions between quantum dots and antibiotic molecules. This step was performed using the GPAW framework [12] with the linear combination of atomic orbitals (LCAO) calculation mode, considering the ground state for the system of surface and adsorbate, as well as the molecules and quantum dots separately.

2.3. Calculation of Adsorption Energies in Gas:

First, adsorption energies were calculated for the relaxed structures in the gas phase. This involved determining the energy difference between the isolated quantum dot and antibiotic molecule and the combined system [13].

$$E_{ads} = E_{complex} - (E_{surface} + E_{adsorbate}) \tag{1}$$

Where:

- $E_{complex}$ is the total energy of the adsorbate-quantum dot system.

- $E_{surface}$ is the energy of the isolated quantum dot.

- $E_{adsorbate}$ is the energy of the isolated adsorbate.

The calculations were performed using different exchange-correlation functionals to account for van der Waals interactions, which are essential for accurately predicting the properties of materials, especially those involving non-covalent interactions. Traditional DFT methods often fail to capture these interactions, leading to inaccuracies in calculated properties such as adsorption energies and structural parameters [14]. Among them, we have the Basis set superposition error (BSSE), which arises in quantum chemistry when the energy of a molecular system (especially dimers or complexes) is calculated using basis sets that are not complete. When using a finite basis set, the computed interaction energy can be artificially lowered because the basis set used for a given monomer does not fully account for the basis functions that would be available in the presence of the other monomer. Essentially, each monomer "benefits" from the virtual orbitals of its partner, leading to an apparent reduction in energy which does not represent the true interaction energy when calculated accurately with a complete basis set [15]. To analyze the importance of these corrections, the calculations were performed using the PBE exchange and correlation functional, with van der Waals corrections added through the DFDT3 functional [16]. Given that, the adjusted energy calculation is given by

5

$$E_{total} = E_{ads} + E_{vdW} \qquad (2)$$

Where the E_{vdW} correction is being calculated with

$$E_{vdW} = E_{complex}(DFTD3) - E_{surf}(DFTD3) - E_{adsorbate}(DFTD3) \qquad (3)$$

So this way, to the initial adsorption eneMacLoughlin2024rgy is added the energy correction alculated through van Der Waals functional.

2.4. Calculation of Adsorption Energies in Solvation:

To simulate more realistic environmental conditions, adsorption energies were also calculated in the presence of a solvent. This step involved using solvation models to account for the interactions between the quantum dots, antibiotic molecules, and the solvent. Efficient implicit solvation models, such as the analytical linearized Poisson-Boltzmann (ALPB) model, are used in semiempirical methods to account for solvation effects. These models provide accurate solvation energies and are computationally efficient, making them suitable for a wide range of systems [17].

3. Results

3.1. Adsorption Dynamics:

During the relaxation calculations, the dynamics of the adsorbate were assessed to determine the most favorable sites for adsorption. However, it was observed that, for each of the quantum dots and configurations, the molecule remained at the original site. The interaction was instead reflected in small deformations in the structure of the surfaces. Accurate start and end points improve the reliability of molecular dynamics simulations and theoretical models, allowing for better predictions of adsorption behavior in various environments, such as liquid-solid interfaces or complex surfaces [18] [19].
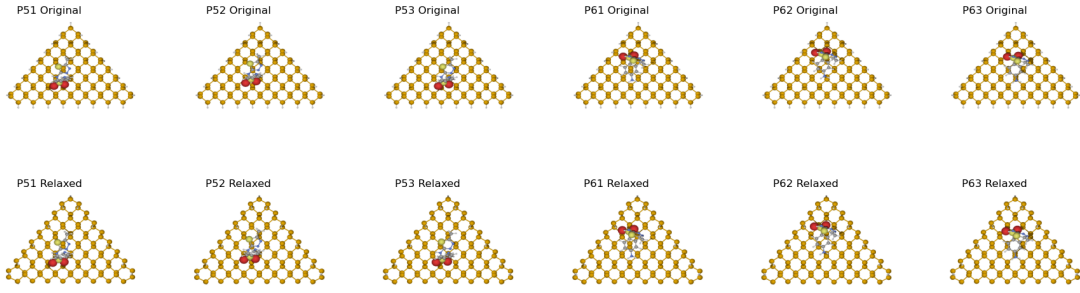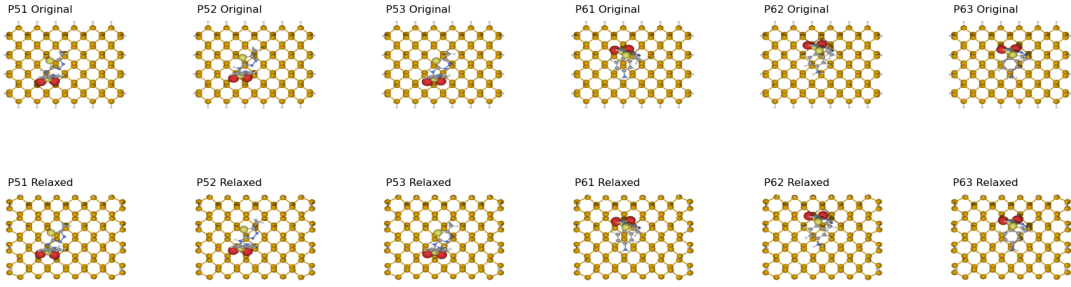
P51 Original   P52 Original   P53 Original   P61 Original   P62 Original   P63 Original

P51 Relaxed   P52 Relaxed   P53 Relaxed   P61 Relaxed   P62 Relaxed   P63 Relaxed

Figure 3: BPTQ configuration

P51 Original   P52 Original   P53 Original   P61 Original   P62 Original   P63 Original

P51 Relaxed   P52 Relaxed   P53 Relaxed   P61 Relaxed   P62 Relaxed   P63 Relaxed

Figure 4: BPSQ configuration

P51 Original   P52 Original   P53 Original   P61 Original   P62 Original   P63 Original

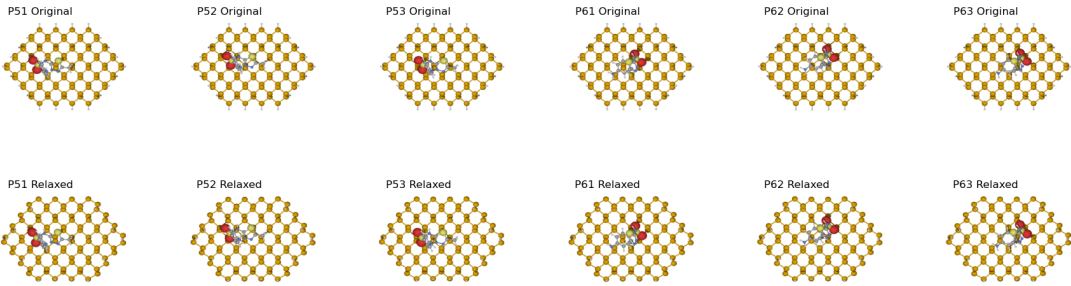P51 Relaxed   P52 Relaxed   P53 Relaxed   P61 Relaxed   P62 Relaxed   P63 Relaxed

Figure 5: BPHQ configuration

Figure 6: Begin and end point for every configuration over every quantum dot

7

3.1.1. Structural Stability Assessment

The comparative visualization in Figure **??** reveals three key findings regarding the relaxation process:

- **Lattice Invariance**: The substrate lattice parameters remain unchanged, with negligible variation in interatomic distances.

- **Adsorbate Stationarity**: Adsorbed sulfamethazine molecules exhibit minimal displacement.

- **Site Preservation**: All molecular configurations maintain their original adsorption sites (top/bridge/hollow) with minimal positional deviations.

3.1.2. Implications of Structural Rigidity

The observed stability suggests:

1. **Near-Equilibrium Initial Conditions**: The pre-relaxation structures were already within the local energy minimum [20].
2. **Symmetry-Governed Stability**: The symmetry of both phosphorene quantum dots and sulfamethazine molecules appears to minimize configurational degeneracy [21].
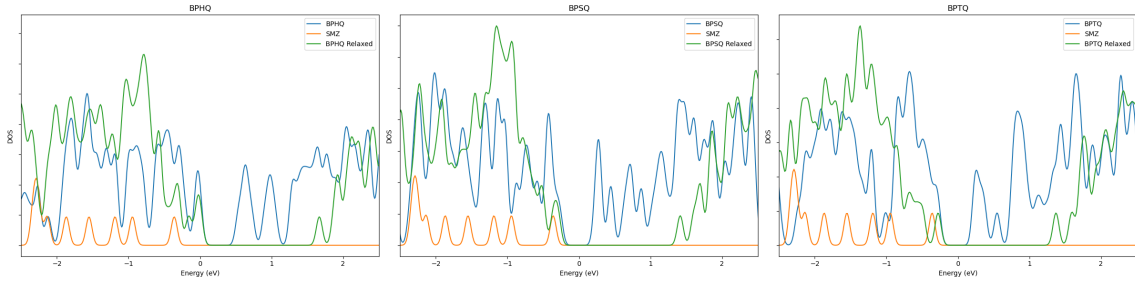
3.2. Density of states

Figure 7: Density of States for the configurations with the strongest adsorption energy. Green curve represents the DoS of the relaxed total system with the adsorbate and the molecule. Orange and blue represent the isolateds molecule and surface respectively.

The green DOS includes both the main molecule and SMZ, meaning the electronic states arise from both species interacting. The trend is consistent for BPHQ, BPSQ, and BPTQ, meaning the hybridization effect between each of these molecules and SMZ follows a similar pattern.

The most noticeable differences appear near the Fermi level (E 0 eV), which suggests that SMZ could alter the transport or conductivity properties of the system.

In certain energy regions, the green curve has features that do not appear in the blue curve, meaning new electronic states emerge in the presence of SMZ.

3.3. Adsorption energies

Table 1: Adsorption energy values for SMZ on PQDs

-	vdW-DF2		DFTD3	
Configuration	Eads Gas (eV)	Eads Water (eV)	Eads Gas (eV)	Eads Water (eV)
BPSQ-SMZ-P51	-0.691	-0.566	-0,781	-0,647
BPSQ-SMZ-P52	-0.696	-0,547	-0,757	-0,606
BPSQ-SMZ-P53	-0.681	-0,543	-0,770	-0,638
BPSQ-SMZ-P61	-0.668	-0,646	-0,862	-0,782
BPSQ-SMZ-P62	-0.715	-0,606	-0,830	-0,700
BPSQ-SMZ-P63	-0.618	-0,583	-0,759	-0,707
BPHQ-SMZ-P51	-0.668	-0,531	-0,828	-0,670
BPHQ-SMZ-P52	-0.659	-0,517	-0,676	-0,587
BPHQ-SMZ-P53	-0.649	-0,511	-0,669	-0,561
BPHQ-SMZ-P61	-0.746	-0,629	-0,799	-0,686
BPHQ-SMZ-P62	-0.654	-0,602	-0,687	-0,656
BPHQ-SMZ-P63	-0.671	-0,578	-0,762	-0,695
BPTQ-SMZ-P51	-0.635	-0,489	-0,753	-0,608
BPTQ-SMZ-P52	-0.621	-0,452	-0,719	-0,561
BPTQ-SMZ-P53	-0.638	-0,456	-0,767	-0,604
BPTQ-SMZ-P61	-0.709	-0,557	-0,910	-0,751
BPTQ-SMZ-P62	-0.733	-0,567	-0,844	-0,689
BPTQ-SMZ-P63	-0.661	-0,534	-0,847	-0,706

The calculated adsorption energy values, ranging from -0.452 to -0.910 eV, confirm that phosphorene quantum dots (PQDs) exhibit strong interactions with sulfamethazine (SMZ). The negative values indicate energetically favorable adsorption across all configurations [22]. Table 2 summarizes the most and least stable configurations:

Table 2: Extreme adsorption energy values for SMZ on PQDs

Property	Configuration	Functional	Phase	E_{ads} (eV)
Strongest adsorption	BPTQ-SMZ-P61	DFTD3	Gas	-0.910
Strongest in water	BPSQ-SMZ-P61	DFTD3	Water	-0.782
Weakest adsorption	BPTQ-SMZ-P52	vdW-DF2	Gas	-0.621
Weakest in water	BPTQ-SMZ-P52	vdW-DF2	Water	-0.452

3.4. Key Trends and Observations

3.4.1. Effect of van der Waals Corrections

The choice of dispersion correction significantly impacts the results:

- DFTD3 predicts consistently stronger adsorption than vdW-DF2 (e.g., BPTQ-SMZ-P61: -0.709 eV vs -0.910 eV in gas phase)

- Energy differences of 10–25% highlight the importance of proper dispersion treatment

3.4.2. Solvent Effects

The aqueous environment reduces adsorption strength:

- Energies are 5–30% weaker in water (e.g., BPTQ-SMZ-P51: -0.753 eV $\rightarrow$ -0.608 eV)

- Exception: BPSQ-SMZ-P61 shows minimal reduction (-0.668 eV $\rightarrow$ -0.646 eV), suggesting particular stability

3.4.3. Structural Dependencies

The data reveal clear structural trends:

- **PQD Geometry**:
  - Triangular (BPTQ) shows strongest adsorption (e.g., -0.910 eV for P61)
  - Hexagonal (BPHQ) intermediate (-0.799 eV)
  - Square (BPSQ) most consistent across configurations

- **Binding Site Preference**:
  - Six-membered ring (P6X) generally outperforms five-membered (P5X)
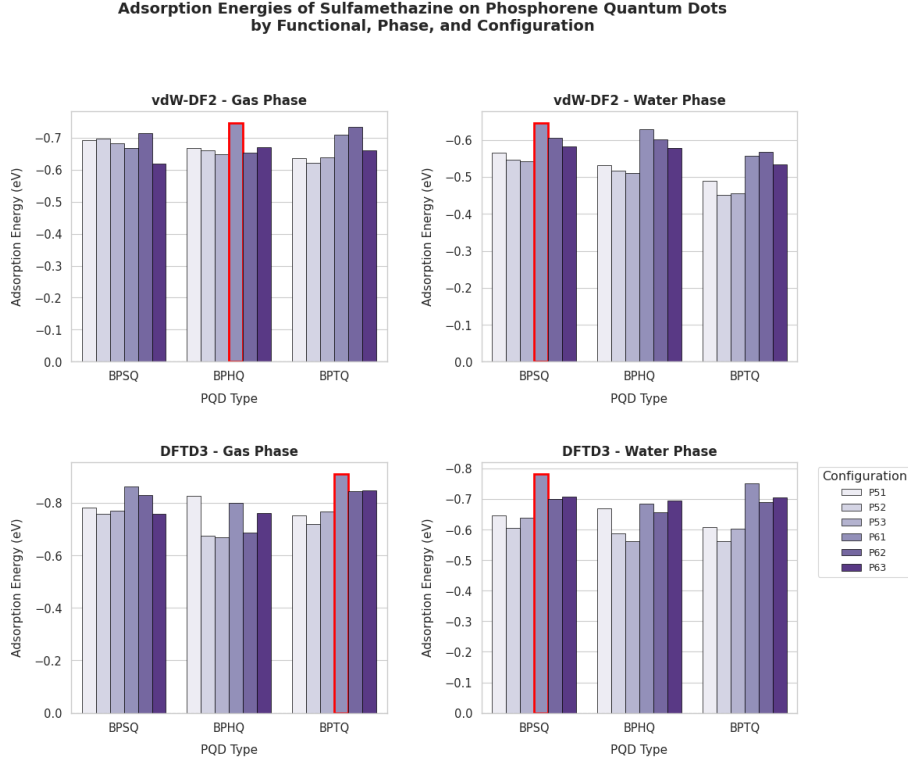 - Hollow sites (P53/P63) more stable than top/bridge sites in water

Adsorption Energies of Sulfamethazine on Phosphorene Quantum Dots by Functional, Phase, and Configuration

Figure 8: Comparison of adsorption energies by PQD geometry and binding site

3.5. Implications for Applications

The results suggest several important considerations for practical implementation:

- Triangular PQDs (BPTQ) with six-membered ring adsorption (P61/P63) are optimal candidates

- The robustness of BPSQ configurations in aqueous environments makes them attractive for water treatment

- DFTD3 should be used for accurate adsorption energy predictions

4. Conclusions

Efficacy of Phosphorene Quantum Dots (PQDs) for Sulfonamide Adsorption. The study demonstrates that phosphorene quantum dots (PQDs) exhibit significant potential for adsorbing sulfonamide antibiotics from aqueous environments. The calculated adsorption energies, particularly when accounting for van der Waals inter-

actions, suggest strong interactions between PQDs and sulfonamide molecules. This highlights PQDs as promising candidates for water decontamination technologies, especially in scenarios where low-concentration pollutants persist.

DFTD3-calculated adsorption energies reveal that triangular PQDs (BPTQ) with six-membered ring orientations (e.g., P61) exhibit the strongest affinity for sulfamethazine (0.910 eV in gas phase), making them optimal for antibiotic capture.

Solvation reduces adsorption energies by up to 30%, but configurations like BPSQ-SMZ-P61 maintain robustness (0.782 eV in water), highlighting their potential for real-world water remediation.

The dominance of hollow sites and six-membered ring interactions underscores the importance of atomic-scale tailoring in PQD design for pollutant removal.

Impact of Solvation and Environmental Conditions The inclusion of solvation models in the calculations provided insights into the adsorption behavior under realistic environmental conditions. While the gas-phase results were informative, the solvation studies are crucial for translating these findings into practical applications, as they account for the complex interactions in aqueous systems. Future work could explore the effects of varying pH, temperature, and ionic strength on adsorption efficiency.

Compared to other 2D materials and biochar-based solutions, PQDs offer unique advantages, such as tunable electronic properties and high surface-to-volume ratios. The study's results align with emerging research on 2D materials but emphasize the distinct potential of PQDs due to their zero-dimensional nanostructure and versatility in forming heterostructures.

To bridge the gap between theoretical predictions and practical applications, experimental validation of these computational findings is essential. Additionally, investigating the recyclability and stability of PQDs in real-world water treatment systems could further validate their suitability for large-scale environmental remediation.

References

[1] T. M. Mac Loughlin, Ma F. Bahl, F. M. Flores, C. D. Apartin, D. J.G. Marino, and Ma L. Peluso. Assessment of sulfonamide contamination in aquatic environments: A first report for argentina and environmental risk assessment. *Science of the Total Environment*, 934, 7 2024.

[2] Weiyan Duan, Hongwu Cui, Xinyu Jia, and Xiao Huang. Occurrence and ecotoxicity of sulfonamides in the aquatic environment: A review, 5 2022.

[3] Chang-Mao Hung, Chiu-Wen Chen, C. Huang, Su Shiung Lam, and C. Dong. Peroxymonosulfate activation by a metal-free biochar for sulfonamide antibiotic removal in water and associated bacterial community composition. *Bioresource technology*, page 126082, 2021.

[4] B. Gámiz, P. Velarde, K. Spokas, and L. Cox. The role of nanoengineered biochar activated with fe for sulfanilamide removal from soils and water. *Molecules*, 27, 2022.

[5] Shihai Cao, Yu Zhang, Nannan He, Jing Wang, Huan Chen, and Fang Jiang. Metal-free 2d/2d heterojunction of covalent triazine-based frameworks/graphitic carbon nitride with enhanced interfacial charge separation for highly efficient photocatalytic elimination of antibiotic pollutants. *Journal of hazardous materials*, 391:122204, 2020.

[6] Arumugam Manikandan, Yu Ze Chen, Chih Chiang Shen, Chin Wei Sher, Hao Chung Kuo, and Yu Lun Chueh. A critical review on two-dimensional quantum dots (2d qds): From synthesis toward applications in energy and optoelectronics, 11 2019.

[7] Jiaxuan Xiao, Xialin Hu, Kun Wang, Y. Zou, Eric Gyimah, S. Yakubu, and Zhen Zhang. A novel signal amplification strategy based on the competitive reaction between 2d cu-tcpp(fe) and polyethyleneimine (pei) in the application of an enzyme-free and ultrasensitive electrochemical immunosensor for sulfonamide detection. *Biosensors bioelectronics*, page 111883, 2019.

[8] Hazem Abdelsalam, Vasil A. Saroka, and Waleed Othman Younis. Phosphorene quantum dot electronic properties and gas sensing. *Physica E: Low-Dimensional Systems and Nanostructures*, 107:105–109, 3 2019.

[9] Lei Zhou, Xuerui Yang, Yuefei Ji, and Jie Wei. Sulfate radical-based oxidation of the antibiotics sulfamethoxazole, sulfisoxazole, sulfathiazole, and sulfamethizole: The role of five-membered heterocyclic rings. *The Science of the total environment*, 692:201–208, 2019.

[10] Ask Hjorth Larsen, Jens Jørgen Mortensen, Jakob Blomqvist, Ivano E Castelli, Rune Christensen, Marcin Dułak, Jesper Friis, Michael N Groves, Bjørk Hammer, Cory Hargus, Eric D Hermes, Paul C Jennings, Peter Bjerre Jensen, James Kermode, John R Kitchin, Esben Leonhard Kolsbjerg, Joseph Kubal, Kristen Kaasbjerg, Steen Lysgaard, Jón Bergmann Maronsson, Tristan Maxson, Thomas Olsen, Lars Pastewka, Andrew Peterson, Carsten Rostgaard, Jakob Schiøtz, Ole Schütt, Mikkel Strange, Kristian S Thygesen, Tejs Vegge, Lasse Vilhelmsen, Michael Walter, Zhenhua Zeng, and Karsten W Jacobsen. The atomic simulation environment—a python library for working with atoms. *Journal of Physics: Condensed Matter*, 29(27):273002, jun 2017.

[11] Zhenzi Yu, Dylan M. Anstine, S. E. Boulfelfel, Chenkai Gu, C. Colina, and D. Sholl. Incorporating flexibility effects into metal-organic framework adsorption simulations using different models. *ACS applied materials interfaces*, 2021.

[12] Jens Jørgen Mortensen, Ask Hjorth Larsen, Mikael Kuisma, Aleksei V. Ivanov, Alireza Taghizadeh, Andrew Peterson, Anubhab Haldar, Asmus Ougaard Dohn, Christian Schäfer, Elvar Örn Jónsson, Eric D. Hermes, Fredrik Andreas Nilsson, Georg Kastlunger, Gianluca Levi, Hannes Jónsson, Hannu Häkkinen, Jakub Fojt, Jiban Kangsabanik, Joachim Sødequist, Jouko Lehtomäki, Julian Heske, Jussi Enkovaara, Kirsten Trøstrup Winther, Marcin Dulak, Marko M. Melander, Martin Ovesen, Martti Louhivuori, Michael Walter, Morten Gjerding, Olga Lopez-Acevedo, Paul Erhart, Robert Warmbier, Rolf Würdemann, Sami Kaappa, Simone Latini, Tara Maria Boland, Thomas Bligaard, Thorbjørn Skovhus, Toma Susi, Tristan Maxson, Tuomas Rossi, Xi Chen, Yorick Leonard A. Schmerwitz, Jakob Schiøtz, Thomas Olsen, Karsten Wedel Jacobsen, and Kristian Sommer Thygesen. Gpaw: An open python package for electronic structure calculations. *Journal of Chemical Physics*, 160, 3 2024.

[13] J. D. Correa, Leonor Chico, V. Nuñez, S. Bravo, and M. Pacheco. Gas sensing characteristics of two-dimensional palladium-based penta-materials. *Sensors and Actuators: A. Physical*, 368:115113, 2024.

[14] John Radly M Sevilla and D. Putungan. Graphene-hexagonal boron nitride van

der waals heterostructures: an examination of the effects of different van der waals corrections. *Materials Research Express*, 8, 2021.

[15] Maciej Gutowski and Grzegorz Chalasinski. Critical evaluation of some computational approaches to the problem of basis set superposition error. *Journal of Chemical Physics*, 98(7):5540–5557, 1993.

[16] David Mahlberg, S. Sakong, Katrin Forster-Tonigold, and A. Gross. Improved dft adsorption energies with semiempirical dispersion corrections. *Journal of chemical theory and computation*, 15 5:3250–3259, 2019.

[17] S. Ehlert, M. Stahn, S. Spicher, and S. Grimme. Robust and efficient implicit solvation model for fast semiempirical methods. *Journal of chemical theory and computation*, 2021.

[18] Nikoleta Ivanova, Vasil Karastoyanov, I. Betova, and M. Bojinov. Study of ammonia adsorption on magnetite surfaces with molecular dynamics simulations. *Molecules*, 29, 2024.

[19] M. Cazzaniga, M. Micciarelli, F. Moriggi, A. Mahmoud, F. Gabas, and M. Ceotto. Anharmonic calculations of vibrational spectra for molecular adsorbates: A divide-and-conquer semiclassical molecular dynamics approach. *The Journal of chemical physics*, 152 10:104104, 2020.

[20] J. Alamatian. Displacement-based methods for calculating the buckling load and tracing the post-buckling regions with dynamic relaxation method. *Computers Structures*, 114:84–97, 2013.

[21] Kai-Yu Yang, Liwei Liu, Lizhi Zhang, W. Xiao, X. Fei, Hui Chen, S. Du, K. Ernst, and Hongjun Gao. Reversible achiral-to-chiral switching of single mn–phthalocyanine molecules by thermal hydrogenation and inelastic electron tunneling dehydrogenation. *ACS nano*, 8 3:2246–51, 2014.

[22] M. Khnifira, A. Mahsoune, M. E. Belghiti, L. Khamar, M. Sadiq, M. Abdennouri, and Noureddine Barka. Combined dft and md simulation approach for the study of so2 and co2 adsorption on graphite (111) surface in aqueous medium. *Current Research in Green and Sustainable Chemistry*, 2021.